RSC Advances

ROYAL SOCIETY OF CHEMISTRY

www.rsc.org/advances

RSC Advances

RSC Publishing

ARTICLE

$Ce_{0.9}Gd_{0.1}O_{2-\delta}$ Membranes Coated With Porous $Ba_{0.5}Sr_{0.5}Co_{0.8}Fe_{0.2}O_{3-\delta}$ for Oxygen Separation

Cite this: DOI: 10.1039/xoxxoooooox

Chi Zhang, Ran Ran, Gia Hung Pham, Kun Zhang, Jian Liu, Shaomin Liu*

Received ooth January 2012,
Accepted ooth January 2012

DOI: 10.1039/xoxxoooooox

www.rsc.org/

Robust oxygen ion-conducting membranes based on doped-ceria oxides can be used as oxygen permeation membranes via the short circuit to provide the required electronic conduction. Previous studies used expensive noble metals to be coated on both surface sides of the ion conducting electrolyte membrane as the electronic conducting phase to fulfil the functions for electron shuttling between the two membrane surfaces required for the oxygen reduction and oxidation. During the membrane operation, the atmosphere surrounding the two membrane sides is different with feed side exposing to air and the permeate side possibly confronting CO_2 or reducing gases like CH_4 or H_2. At high operating temperature, such different gas atmosphere poses different requirements on the material choice to prepare the membranes thus leaving space for further optimisation to reduce the material cost. In this work, a novel $Ce_{0.9}Gd_{0.1}O_{2-\delta}$ (GDC) with cost-effective mixed conductive $Ba_{0.5}Sr_{0.5}Co_{0.8}Fe_{0.2}O_{3-\delta}$ (BSCF) layer to replace the preciously employed noble metal layer on the membrane surface facing the air atmosphere was developed to deliver a highly stable oxygen flux for possible applications in clean energy or membrane reactors for chemical synthesis. Further on, we noted that the membranes coated with BSCF improved the oxygen fluxes compared to the membranes coated with pure silver. A triple phase boundary (TPB) theory has been put forward to deeply explain the observed improvement on oxygen flux values.

1 Introduction

The annual global oxygen production is predicted to reach hundreds of millions of tons from air separation and contributes the largest section in the industrial gases market with sales worthy of more than $5 billion in 2014.[1] Oxygen has wide applications touching almost every sector of the global economy from a variety of industries like metal manufacturing, chemicals, pharmaceuticals, petroleum, glass, cement, ceramics, pulp/paper manufacturing and others. Currently in oxygen market, the power generation industry is only sharing 4%.[2] However, in the near future, this market for energy will be massively expanded by the required deployment of clean energy technologies like IGCC and Oxyfuel projects to decrease the CO_2 emission; these clean energy projects require the oxygen as the feed gas. Estimation indicates that, in 2040, the energy industry sector will occupy the oxygen market by 60% requiring approximately two million tons per day.[2] Currently, the industrial tonnage oxygen is produced at a lower purity (<93%) with intermediate scale by pressure swing adsorption or a high purity (>93%) and large scale (i.e. >1000 tons per day) by cryogenic distillation. Both methods are expensive; in particular, the cryogenic distillation by cooling down the air to minus 185^{o}C, a very mature technique, has been used since the early 1900s without much space for improvement. These conventional high-cost oxygen production technologies largely prohibit the clean energy technology application. To battle the extreme climate change via carbon capture and storage (CCS), our contemporary society urgently needs to make the oxygen production technology more cost-effective to enable these clean energy schemes. Among the emerging new technologies, ceramic membrane technology offers the greatest potential due to its energy efficiency and less capital investment. Starting from 1997, Air Products and US DoE have initiated the longest and biggest investment worthy of $150 million to advance this novel technique often referred as revolutionary ion transporting membrane (ITM) technology.[3] The associated research was actually started in 1980s when the appreciable oxygen permeation flux through dense perovskite membrane in a general formula of $La_{1-x}Sr_xCo_{1-y}Fe_yO_{3-\delta}$ was reported by Teraoka and co-workers.[4] Since then, a variety of perovskite ceramics with oxygen permeation properties have been encouraged with a general formula $ABO_{3-\delta}$ where A and B sites can be individually or jointly occupied by La, Sr, Ba, Ca, or Zr and Mg, Al, Ti, Cr, Mn, Fe, Co, Ni, Cu, Ga, Zr, Ta, W, Sc or Zn, respectively.[5-20] Due to the structural flexibility of the perovskite structure, 90% of the metals listed in the element periodic table have been attempted for perovskite structure synthesis.[21] One common feature of these membranes is that they are able to simultaneously conduct both oxygen ions and electrons at elevated temperatures and thereby classified as mixed ionic and electronic conducting (MIEC) ceramic membranes with working principle schematically shown in Fig. 1a. When exposed to oxygen partial pressure gradient, oxygen

can permeate through these perovskite membranes through surface transferring reactions and bulk diffusion without the necessity for external electric loadings compared to pure ionic conductors (Fig. 1b).[22] To sustain a high oxygen flux, the membranes must possess not only sufficient ionic and electronic conductivities but also good surface reactions for oxygen exchange between its gaseous molecular state and solid lattice oxygen. An apparent progress has been evidenced in the past two decades during material optimisation and scale up for engineering applications. For instance, oxygen flux up to 14.5 ml min^{-1} cm^{-2} at 950°C was achieved on thin $Ba_{0.5}Sr_{0.5}Co_{0.8}Fe_{0.2}O_{3-\delta}$ (BSCF) membrane supported on hollow fibre geometry under the oxygen pressure gradient created by non-pressurized air and sweep gas.[23] Long term operational stability over thousands of hours has been achieved on BSCF and $La_{0.6}Sr_{0.4}Co_{0.2}Fe_{0.8}O_{3-\delta}$ (LSCF) membranes for oxygen production under vacuum operation or non-reacting sweep gas models.[5,24,25] Encouraging news also come from Air Products that their ITM project has been advanced to Phase-5 testing the oxygen producing capability of 2000 tons per day.[26] Inspired by the success of membrane technology for pure oxygen production, the research communities have initiated another ambitious project to develop ITM syngas to combine the air separation and gas oxidation in a single unit with working principles displayed in Fig. 1c. Once successful, this novel technology will greatly advance our current petrochemical industries and clean energy deployment as it can save 20 to 30% capital cost for the overall synthesis gas and H_2 production.[3] In particular, it will help to improve the viability of the Oxyfuel project by retrofitting the existing power plants rather than setting up the new boiler system.[26]

These ambitious targets pose stricter requirement on the membrane material stability. As shown in Fig. 1c, the permeate side of the membrane would face the reducing gases like CH_4 or acid gases like CO_2 for high temperature reactions. However, all these developed membranes cannot survive in such harsh reducing or acid gas atmosphere at high temperatures for the long term due to fact that these perovskite oxides are easily damaged by the reaction with these gases.[27,28] Fortunately, robust membranes with sufficient stability to endure these gases can be found from fluorite-type ion conducting ceramics such as yttria-stabilized zirconia (YSZ), gadolinium (or samaria)-doped ceria (GDC/SDC), which is evidenced by the wide applications in solid oxide fuel cells as the high temperature electrolyte for oxygen ion transport.[29-31] Despite of their proven robustness, their application as oxygen production membrane is quite limited owning to their insufficient electronic conductivity and the associated more complex membrane design via oxygen pump with external electric loadings (Fig. 1b). To simplify the membrane design, researchers have attempted to mix the noble metal powders like Pt, Au, Pd and Ag with YSZ, SDC or GDC to prepare a dual phase membrane in which metal and ion conductor phases can individually transfer oxygen ions and electrons simultaneously. However, it is difficult to guarantee the continuous conducting path for each phase, often leading to super low oxygen fluxes due to the mismatch problem between the two phases.[22] Recently, based on the configuration of solid oxide fuel cell, a novel ion conducting ceramic membrane design with short circuit has been reported.[32] Noble metals, instead of mixing with ceramics, were decorated as a thin coating layer on the ceramic surface. Together with electronic conducting sealant (i.e. Ag paste) as the short circuit, the porous metal layer functions as the continuous electric conducting phase for electrons shuttling between the two membrane surfaces during the oxygen exchange reactions. In the previous research, noble Ag or Pt was decorated on both membrane surfaces as the electronic conducting phase to verify this concept as schematically shown in Fig. 1d,[32,33] but the high cost of these precious metals is a drawback for the future large-scale applications. As aforementioned, some MIEC perovskites are good electronic conductors with sufficient oxygen exchange kinetics and high stability in air atmosphere, thus they can be used as the coating material to reduce the material cost by replacing the Ag or Pt layer in the air (feed) side of the GDC, YSZ or SDC membranes during air separation.

In this report, we tested this membrane design using the porous MIEC perovskite to coat the membrane surface facing the air side but leaving the permeate side still with precious metal (Ag) coating to confront the sweep gas containing CO_2. To test this hypothesis, $Ba_{0.5}Sr_{0.5}Co_{0.8}Fe_{0.2}O_{3-\delta}$ (BSCF) was used as the perovskite phase and ion conducting membrane was selected from gadolinium-doped ceria (GDC). In order to fully understand the effects of different electronic conducing phases from ceramics or precious metals on the overall oxygen transport, some membrane samples were coated on both sides with BSCF and performances were compared with that from Ag coated membranes.

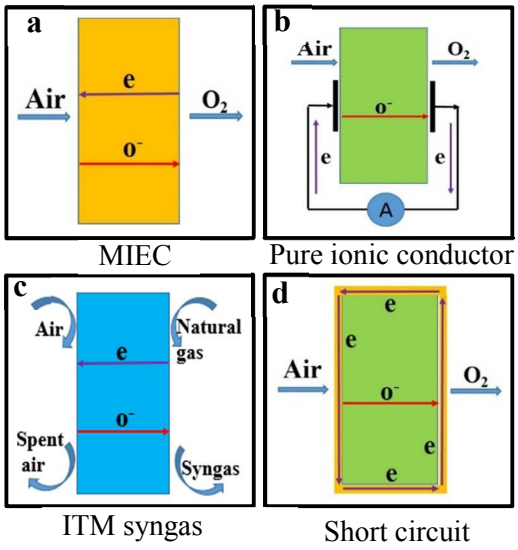

Fig. 1 Schematic diagram of different oxygen permeation membrane design models. (a) Mixed ionic-electronic conducting oxide membranes; (b) Pure oxygen ionic conducting membranes with external power; (c) Ion transport membrane (ITM) reactors for syngas production; (d) Pure oxygen ionic conducting membranes with short-circuit coating.

2 Experimental

$Ce_{0.9}Gd_{0.1}O_{2-\delta}$ (GDC) and $Ba_{0.5}Sr_{0.5}Co_{0.8}Fe_{0.2}O_{3-\delta}$ (BSCF) ceramic oxides were synthesized by a combined EDTA-citrate complexing sol-gel process. The metal element precursors are from their nitrate salts of $Ce(NO_3)_2{\cdot}xH_2O$, $Gd(NO_3)_2{\cdot}xH_2O$, $Ba(NO_3)_2$, $Sr(NO_3)_2$,

$Co(NO_3)_2 \cdot 6H_2O$ and $Fe(NO_3)_3 \cdot 9H_2O$, which were purchased from Aldrich and used as received. The stoichiometric quantities of metal nitrates in aqueous solution were dissolved in distilled water. Then EDTA and citric acid were added as the complexing agents. $NH_3 \cdot H_2O$ was added into the above solution to control the pH value at around 6 ~ 8. The molar ratios of total metal ions, EDTA, citric acid were controlled at 1:1:2. The solution was heated at 90 °C to evaporate the water and obtain a transparent gel. The gel was pre-fired at 250 °C and heated at 700 or 950°C for GDC or BSCF, respectively, in air for 5 h to get the ceramic powder with desired structure.

To fabricate the membrane, 0.4 grams of the ceramic powder was pressed into a disk-shaped membrane in a stainless steel mould (15.0 mm in diameter) under a hydraulic pressure of approximately 1.5×10^8 Pa. These green membranes (~0.8 mm in thickness) were further sintered at 1350 °C for 10 h at a ramping/cooling rate of 2°C/min. BSCF was dispersed in an ink vehicle mixed solution and then was coated to the surfaces of some GDC membranes by brush painting for at least 3 times followed by calcination at 1000 °C in air for 2 h. Silver slurry was applied to the surface of other GDC membranes by a similar brush painting and subsequently calcined at 600 °C for 2 h.

To investigate the phase composition of membranes, the XRD analysis was carried out by a Bruker D8 Advance X-ray diffractometer using Cu Ka radiation generated at 40 kV and 30 mA. Scanning Electron Microscopy (SEM) images were obtained using a Zeiss EVO 40XVP at an accelerating voltage of 15 kV.

A Shimadzu 2014A gas chromatography (GC) equipped with a 5 Å capillary molecule column and thermal conductivity detector for quantitative oxygen concentration analysis was used during the high temperature oxygen permeation test. To set up the permeation cell, a silver paste was applied as the sealant to fix the disk membrane onto a dense quartz tube. The effective membrane area was about 0.45 cm^2. The partial pressure of oxygen in the feed stream was 0.21 atm. Helium was applied as the sweep gas to bring the permeated oxygen to the GC for concentration analysis. Assuming that leakage of nitrogen and oxygen through pores or cracks is in accordance with Knudsen diffusion, the fluxes of leaked N_2 and O_2 are related by

$$J_{N_2}^{Leak} : J_{O_2}^{Leak} = \sqrt{32/28} \times 0.79 : 0.21 = 4.02.$$

The O_2 permeation flux was then calculated by subtracting the leaked oxygen using the equation below:

$$J_{O_2}(\text{ml min}^{-1}\ \text{cm}^{-2}) = \left[C_{O_2} - C_{N_2}/4.02\right] \times \frac{F}{S}$$

where C_{O_2} and C_{N_2} are the measured concentrations of oxygen and nitrogen in the gas on the permeate side, respectively, F is the flow rate of the exit gas on the permeate side (ml min^{-1}), and S is the membrane geometric surface area of the sweep side (cm^2).

3 Results and discussion

To test the phase components of GDC membranes and the coating decorations, XRD analysis was carried out. Fig. 2 shows the typical XRD patterns of the membranes used for oxygen permeation test. As shown in Fig. 2a, the characteristic peaks of GDC are located at the respective 2θ angles of 28° (111), 33° (200), 47° (220), 52° (311), 58° (222), 76° (331) and 79° (420), which agrees with the previously reported.[34,35] Fig. 2b displays the XRD patterns of the GDC with BSCF coating on the surface. All the peaks can be clearly assigned to GDC and BSCF, respectively. No other undesired phases can be observed, which rules out the reaction between these two phases and proves the stable coexistence of GDC and BSCF. Fig. 2c shows that the existence of Ag coating; however, compared to the strong diffraction signal from Ag, GDC peaks are relatively weak thus its observation in Fig. 2c is not as distinguishable as that in Fig. 2a or 2b.

Fig. 3a and b show the SEM images of the surface and cross section views of the pure GDC membrane with the GDC grain size of 0.5-1.0 μm (the inset of Fig. 3a). The dense structure of sintered GDC membrane is observed not only from the surface but also from the cross section view (Fig. 3b) as no apparent porosity can be detected in the SEM image. The BSCF was initially dispersed inside the ink vehicle solution and then coated on the GDC membrane followed by sintering at high temperature to increase the interface adhesion. The SEM of the obtained porous coating structure is displayed in Fig. 3c. As seen, the pore size is in the range of 2-3 μm and the porous BSCF coating layer has the thickness around 5.0 μm as marked by the horizontal line in Fig. 3d; in contrast, the thick supporting bulk layer is the densified GDC structure (as shown in the inset of Fig. 3d). The GDC membrane coated with Ag paste presents a porous structure with the thickness of about 6.0 μm as well (Fig. 3e and f). The porous structure, no matter BSCF or Ag, would be used to promote the oxygen permeation fluxes.[9,32,36]

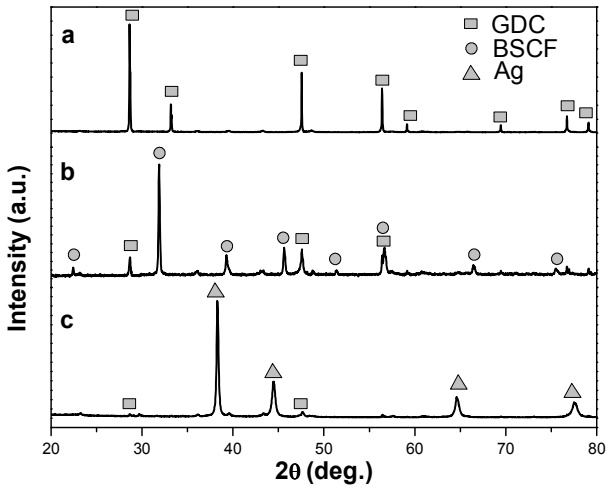

Fig. 2 XRD patterns of (a) GDC, (b) GDC coated with BSCF and (c) GDC coated with Ag.

In order to test the feasibility of the BSCF coating to promote the oxygen transport through the GDC membrane, three typical membranes (Samples a, b and c) with varied coating layers were purposely chosen to display the flux difference based on the similar 0.8 mm thickness of the bulk diffusion GDC layer. All the oxygen permeation tests were repeated for 3 times. Sample-a has Ag coatings on both membrane sides; Sample-b has Ag coating on one side but the other side with BSCF coating; Sample-c has both sides with BSCF coatings. As shown in Fig. 4, the coating of BSCF layer (Sample-b or c) on the membrane significantly improved the oxygen fluxes at relatively similar operating temperatures and sweep gas

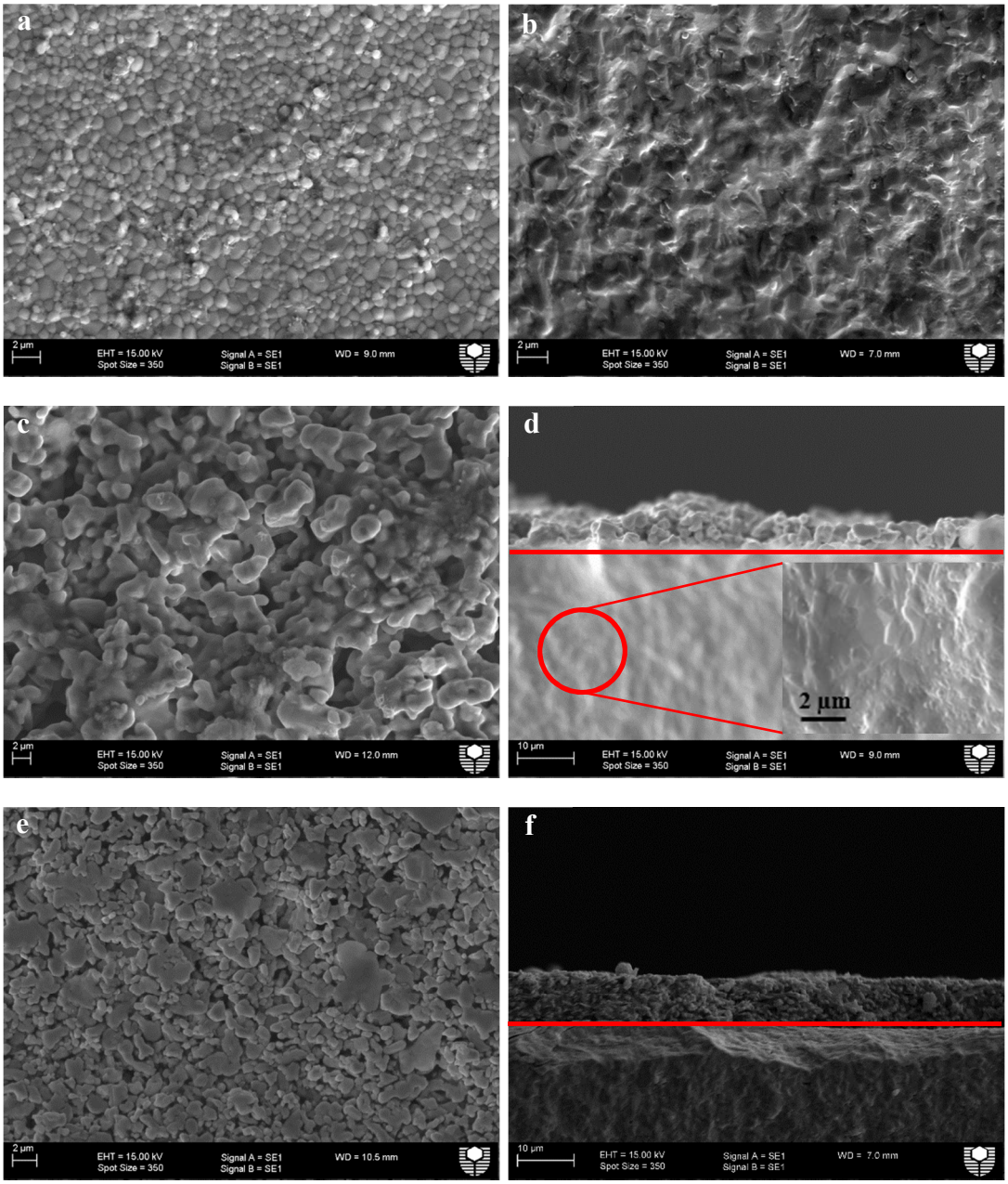

Fig. 3 The SEM images of (a) surface of GDC, (b) cross section of GDC, (c) surface of GDC membrane decorated with BSCF coating, (d) cross section of GDC membrane decorated with BSCF coating, (e) surface of GDC membrane decorated with Ag coating and (f) cross section of GDC membrane decorated with Ag coating.

rate. For example, at 650 °C, the oxygen flux of Sample-a with Ag coating on both membrane sides was 0.017 ml min^{-1} cm^{-2} (Fig. 4a) while the flux of BSCF coating in the permeate side with Ag coating still in feed side (Sample-b) was improved by 16% to 0.02 ml min^{-1} cm^{-2} (Fig. 4b). When both membrane sides were coated by the BSCF layer (Sample-c), the flux was further raised by 27% to 0.023 ml min^{-1} cm^{-2} compared to Sample-a at the operation temperature of 650 °C. When the temperature was continuously rising, the oxygen fluxes of all the three samples had been lifted up compared to that operated on lower temperatures; such promoting effect of temperature on the flux value can be easily interpreted by the temperature activation on the oxygen exchange surface reactions and oxygen ion bulk diffusion. However, a careful inspection of the flux enlargement by the BSCF coating at different temperatures illustrates that at higher temperatures such flux improvement is more distinguishable than that at lower temperatures. For instance, at 800 °C, compared to the flux of 0.043 ml min^{-1} cm^{-2} from Sample-a, the respective fluxes of Samples-b and c were 0.075 and 0.088 ml min^{-1} cm^{-2} with improvement percentage by 42% and 51%, respectively. The relative larger flux improvement with BSCF coating at higher temperatures indicating the percentage of surface reaction resistance

in the overall resistance (surface reaction plus bulk diffusion) to determine the limiting step for oxygen transport gradually increases

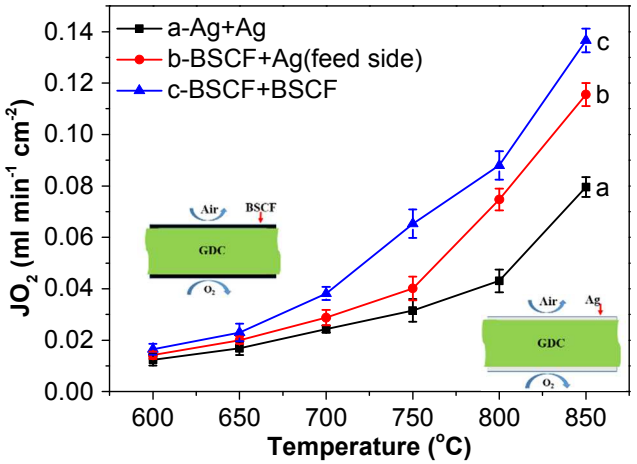

Fig. 4 Oxygen permeation of GDC coated with (a) Ag at both feed side and permeate side, (b) Ag at feed side and BSCF at permeate side and (c) BSCF at both feed side and permeate side. The sweep rate is 100 ml min^{-1}.

with the rise of the operating temperature. However, to theoretically explain the larger oxygen permeation improvement by coating of a mixed conductor like BSCF more than the pure electronic conductor of Ag, we have to resort to the two membrane surface reactions as described as below:

$\frac{1}{2}O_2 + V_O^{\cdot\cdot} + 2e \rightarrow O_O^x$ (air side of the membrane surface) (2);

$O_o^x \rightarrow \frac{1}{2}O_2 + V_O^{\cdot\cdot} + 2e^{\cdot}$ (permeate side of the membrane surface) (3).

where $O_O^{\times}$ stands for lattice oxygen, $V_O^{\bullet\bullet}$ for oxygen vacancy and e for electron. At the membrane surface facing air, molecular oxygen has been reduced to lattice (or ionized) oxygen with the acceptance of electrons. On the other membrane surface facing the sweep gas, molecular oxygen and electrons are released via the lattice oxygen oxidation. Thus, each surface reaction only takes place in their respective triple phase boundary (TPB) area. Just schematically shown in Fig. 5a, when the membrane is coated by Ag, the TPB areas are marked by shapes of pink squares where Ag, GDC and oxygen (or sweep gas He) can meet together to make the surface reactions possible. This requires the Ag coating layer to be continuous, uniform and porous with strong adherence to the GDC surface. However, the Ag coating via brush painting method and high temperature treatment will be agglomerated; in such case, the GDC areas covered by the Ag agglomerates marked by the dotted rectangle would be sacrificed and make no contribution toward the surface reactions. In another word, large Ag particles from the coating layer block the ionic bulk diffusion due to the very limited TPB area. However, such restriction has been removed if the coating layer is replaced by the mixed conductor like BSCF in Fig. 5b where the TPB area has been expanded from the area marked by the pink squares to the entire BSCF particle surface thus improving the oxygen surface reaction kinetics. Of course, BSCF particles should be strongly adhered on the GDC surface to decrease the interface ionic or electron transport resistance. This is the reason that a mixed conductor-BSCF coating on GDC can improve the oxygen permeation flux compared by Ag coating. The similar observation was also made by Yang and co-workers who employed the pulse laser method to deposit the $La_{0.8}Sr_{0.2}CoO_{3-\delta}$ oxides on SDC membrane.[37,38]

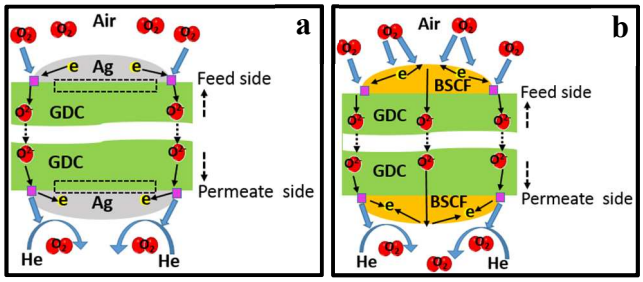

Fig. 5 Schematic diagram showing of the effects of different coatings on the oxygen permeation process (a: pure electronic conductor of Ag; b: mixed conductor of BSCF)

In addition to the temperature activation, Fig. 6 displays another driving force to boost the oxygen flux by increasing the sweep gas flow rate which lowers down the oxygen partial pressure in the permeate side, thus enlarges the oxygen partial pressure gradient. This trend can be easily recognized from the variation trend in Fig. 6. For instance, the oxygen flux through the membrane Sample-c increased noticeably from 1.02 to 1.21 ml min^{-1} cm^{-2}, as the sweep gas rate was changed from 80 to 120 ml min^{-1} at 850°C. Noteworthy is that in this research, the ambient air and He were used as the feed and the sweep gas, respectively, the largest oxygen partial pressure gradient only would reach 0.21/0.001. However, under reaction conditions for industrial applications, the air as the feed gas will be pressurized to 50 atm and the permeated oxygen will be consumed by the reaction so that the oxygen partial pressure gradient can be as large as 10/10^{-16} atm. Under such circumstance, the oxygen flux would be very fast. Thus, the factor that restricts the reaction performance is not oxygen flux but the membrane materials stability under the real applications.

Supposing that the oxygen flux is completely controlled by the bulk diffusion as the membrane surface coating improves oxygen exchange surface reaction kinetics to a minimum resistance, we can estimate the maximum theoretical oxygen flux based on the Wagner equation, $J_{O_2} = \frac{RT}{16F^2L}\sigma_i \ln\frac{P'_{O_2}}{P''_{O_2}}$, where T is the absolute temperature, R is the ideal gas constant, F is the Faraday's constant, L is the thickness of the membrane, σ_i represents the oxygen ion conductivity of GDC, P'_{O_2} and P''_{O_2} represent the oxygen partial pressure at the feed and permeate side.

Table 1. Oxygen ion conductivity and theoretical oxygen permeation flux of GDC membrane coated with BSCF on both sides.

Temp °C	σ_i (S cm^{-1}) [39]	Theoretical J_{O_2} (ml min^{-1}cm^{-2})	Measured J_{O_2} (ml min^{-1}cm^{-2})
600	4.05·10-3	0.018	0.016
650	8.44·10-3	0.039	0.023
700	1.29·10-2	0.063	0.038
750	2.03·10-2	0.104	0.065

A number of researches have been carried out to measure the oxygen ion conductivity of GDC membrane.[39-43] Based on different GDC synthesis methods, there may be a minor difference in

conductivity values. Table 1 shows the oxygen ion conductivity at different temperatures from the literature[39]. The maximum theoretical oxygen fluxes were calculated with results showing in Table 1. Compared with the theoretical oxygen fluxes, the measured fluxes in this work are 10-40% smaller, which indicates that the surface reaction kinetics did contribute a certain resistance to limit the overall oxygen transport.

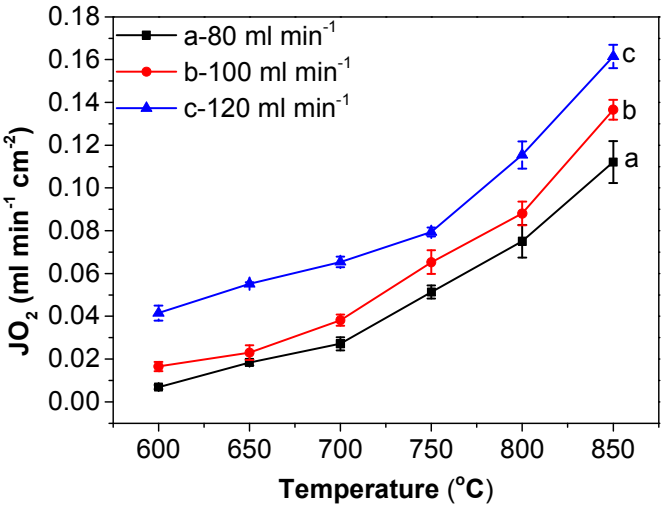

Fig. 6 The effect of sweep gas rate on oxygen permeation fluxes.

Two types of coated GDC membranes (Samples c and d) were tested for a long term by adding CO_2 in the sweep gas on the permeate side. Just as aforementioned, Sample-c has BSCF coatings on both sides of the membrane but for Sample-d GDC was coated by Ag and BSCF layer. Fig. 7 depicts the stability performance tests of the selected two typical membranes. During the test, the BSCF coating side of the membrane (Sample-d) was facing the feed air and the Ag-coating side was confronting the sweep gas with CO_2 content. As expected, the oxygen flux of Sample-c coated on both sides with BSCF layers was suffering a continuing decline when switching the sweep gas from pure He to its mixture with 10% CO_2 (Fig. 7a). At high temperature of 800 ^oC and operated for 600 minutes, the Sample-c lost the flux value by more than 50%; after the sweep gas was changed back to pure helium, the oxygen flux could not be recovered to its original value due to the carbonate formation from the reactions between the alkaline earth metals like Ba/Sr and CO_2.[27,44] In sharp contrast, the Sample-d worked very well under such circumstances. The GDC membrane with coatings of BSCF and Ag displayed very stable oxygen fluxes in He or CO_2 containing mixtures. As can be seen from Fig. 7b, after introducing CO_2 into the He sweep gas, the flux value was marginally lowered but could be maintained at a stable value of 0.044 ml min^{-1} cm^{-2}. The temporary flux decrease with the introduction of CO_2 is due to the stronger CO_2 adsorption than helium to the membrane surface, but not due to the reaction between CO_2 and GDC. The wide application of GDC as solid electrolyte in the solid oxide fuel cells verifies its sufficient chemical stability to withstand the gases like CO_2 and CH_4.[45] Thus, when the sweep gas was switched back to pure He, the oxygen flux could be quickly recovered to the original value.

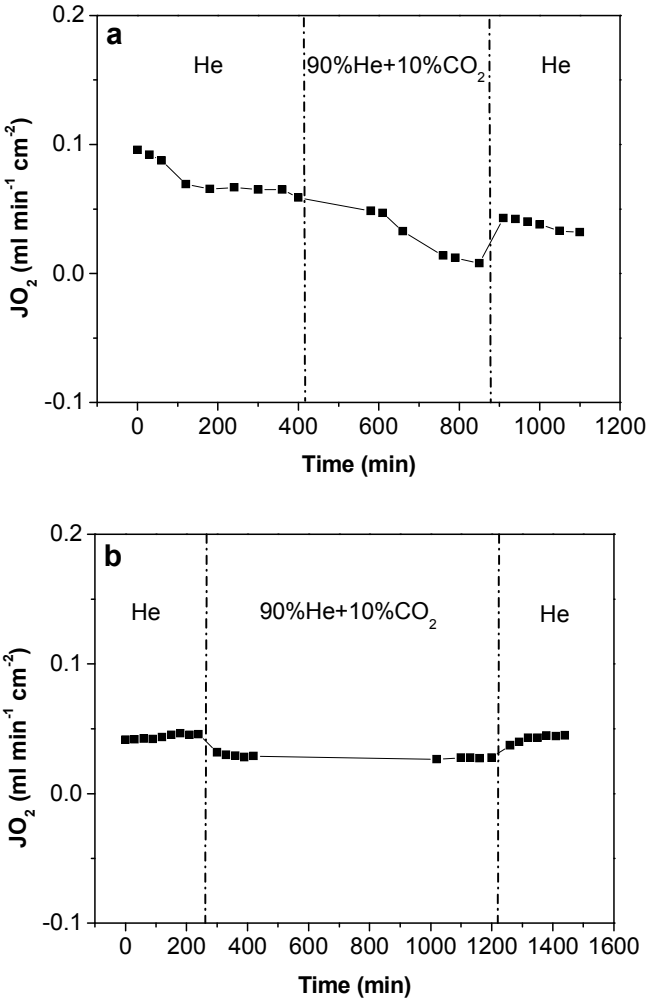

Fig. 7 Long term oxygen permeation tests through GDC membranes coated with (a) BSCF on both sides, (b) BSCF on feed side and Ag on sweep side. The sweep rate is 100 ml min^{-1}.

4 Conclusions

Based on the working principles of solid oxide fuel cells, a short-circuited robust ion conducting ceramic membrane configuration has been recently suggested to conquer the weak stability problem of the state of art ceramic membrane in CO_2 or reducing gas atmosphere at high temperatures.[32] However, the previous design was of high material cost since it used the expensive noble metal on the two membrane sides. This study demonstrated the feasibility of using a cheaper mixed conducting ceramic coating for electronic conduction on the robust ion conducting ceramic membranes for oxygen separation. To illustrate the membrane concept, the gadolinium-doped ceria (GDC), $Ba_{0.5}Sr_{0.5}Co_{0.8}Fe_{0.2}O_{3-\delta}$ (BSCF) or Ag paste were chosen as the ion conducting membrane, surface coating material from the mixed or pure electronic conductor, respectively. Experimental results indicate that the replacement of Ag coating by BSCF on GDC membrane significantly improved the oxygen flux due to the increased triple phase boundary (TPB) area with improved oxygen exchange surface reaction kinetics. The maximum oxygen flux was 0.13 ml min^{-1} cm^{-2} at 850 °C with densified GDC thickness of 0.8 mm and both sides coated by BSCF. The GDC membrane

with BSCF coating facing air and Ag coating exposing to CO_2 mixture worked very stably during the long term permeation test, which enables possible applications in clean energy area like oxyfuel projects and membrane reactors for syngas production.

Acknowledgements

The authors appreciate the financial support provided by the Australian Research Council through the Future Fellow Program (FT12100178). Mr. Chi Zhang acknowledges the PhD scholarship provided by Curtin University.

Notes

[a] Department of Chemical Engineering, Curtin University, Perth, WA 6845, Australia. Tel.: +61892669056; E-mail: shaomin.liu@curtin.edu.au

References

1 PRWeb, http://www.prweb.com/releases/2013/11/prweb11347927, (accessed November 2013).
2 World nuclear association, http://www.world-nuclear.org/info/Energy and-Environment/- Clean-Coal--Technologies/, (accessed May 2014).
3 Ted Foster, Air products, *Air Separation Technology-Ion Transport Membrane (ITM)*, Allentown, 2008.
4 Y. Teraoka, H.M. Zhang, S. Furukawa, N. Yamazoe, *Chem Lett.*, 1985, **14**, 1743.
5 Z.P. Shao, W.S. Yang, Y. Cong, H. Dong, J.H. Tong, G.X. Xiong, *J. Membr. Sci.*, 2000, **172**, 177.
6 Z.B. Zhang, D.J. Chen, Y. Gao, G.M. Yang, F.F. Dong, C. Chen, F. Ciucci, Z.P. Shao, *RSC Adv.*, 2014, **4**, 25924.
7 D.Z. Han, J.H. Wu, Z.F. Yan, K. Zhang, J. Liu, S.M. Liu, *RSC Adv.*, 2014, **4**, 19999.
8 H.H. Wang, R. Wang, D.T. Liang, W.S. Yang, *J. Membr. Sci.*, 2004, **243**, 405.
9 S. Baumann, J.M. Serra, M.P. Lobera, S. Escolástico, F. Schulze Küppers, W.A. Meulenberg, *J. Membr. Sci.*, 2011, **377**, 198.
10 X.Y. Lin, T. Kerstiens, T. Markus, *J. Membr. Sci.*, 2013, **438**, 83.
11 F. Schulze-Küppers, S. Baumann, W.A. Meulenberg, D. Stöver, H.-P. Buchkremer, *J. Membr. Sci.*, 2013, **433**, 121.
12 M. Katsuki, S.R. Wang, M. Dokiya, T. Hashimoto, *Solid State Ionics*, 2003, **156**, 453.
13 J. Luyten, A. Buekenhoudt, W. Adriansens, J. Cooymans, H. Weyten, F. Servaes, R. Leysen, *Solid State Ionics*, 2000, **135**, 637.
14 T. Ramos, A. Atkinson, *Solid State Ionics*, 2004, **170**, 275.
15 Y. Zou, W. Zhou, S.M. Liu, Z.P Shao, *J. Eur. Ceram. Soc.*, 2011, **31**, 2931.
16 B. Meng, Z.G. Wang, Y.Y. Liu, X.Y. Tan, J.C.D. da Costa, S.M. Liu, *Sep. Purif. Technol.*, 2011, **78**, 175.
17 X.Z. Chen, L. Huang, Y.Y. Wei, H.H. Wang, *J. Membr. Sci.*, 2011, **368**, 159.
18 M. Shang, J.H. Tong, R. O'Hayre, *RSC Adv.*, 2013, **3**, 15769.
19 V.V. Kharton, S.B. Li, A.V. Kovalevsky, E.N. Naumovich, *Solid State Ionic*, 1997, **96**, 141.
20 J.X. Yi, S.J. Feng, Y.B. Zuo, W. Liu, C.S. Chen, *Chem. Mater.*, 2005, **17**, 5856.
21 K. Zhang, J. Sunarso, Z. Shao, W. Zhou, C. Sun, S. Wang, S. Liu, *RSC Adv.*, 2011, **1**, 1661.
22 J. Sunarso, W.A. Meulenberg, S. Baumann, J.M. Serra, S. Liu, J.C.D. da Costa, Y.S. Lin, *J. Membr. Sci.*, 2008, **320**, 13.
23 A. Leo, S. Smart, S. Liu, J.C.D da Costa, *J. Membr. Sci.*, 2011, **368**, 64.
24 D. Schlehuber, E. Wessel, L. Singheiser, T. Markus, *J. Membr. Sci.*, 2010, **351**, 16.
25 X. Tan, Z. Wang, B. Meng, X. Meng, K. Li, *J. Membr. Sci.*, 2010, **352**,189.
26 J. Repasky, D. McCarthy, P. Armstrong, M. Carolan, *Workshop on Technology Pathways Forward for Carbon Capture & Storage on Natural Gas Power Systems*, Washington DC, 2014
27 A.Waindich, A. Mobius, M. Müller, *J. Membr. Sci.*, 2009, **337**, 182.
28 J. Yi, M. Schroeder, *J. Membr. Sci.*, 2011, **378**, 163.
29 J. Kim, Y.S. Lin, *J. Membr. Sci.*, 2000, **167**, 123.
30 C.S. Chen, B.A. Boukamp, H.J.M. Bouwmeester, G.Z. Cao, H. Kruidhof, A.J.A. Winnubst, A.J. Burggraaf, *Solid State Ionics*, 1995, **76**, 23.
31 T.J. Mazanec, T.L. Cable, J.G. Frye Jr., *Solid State Ionics*, 1992, **53**, 111.
32 K. Zhang, Z. Shao, C. Li, S. Liu, *Energ. Environ. Sci.*, 2012, **5**, 5257.
33 K. Zhang, L. Liu, Z. Shao, R. Xu, J.C.D. da Costa, S. Wang, S. Liu, *J. Mater. Chem. A*, 2013, **1**, 9150.
34 J. Xue, Q. Liao, Y.Y. Wei, Z. Li, H.H. Wang, *J. Membr. Sci.*, 2013, **443**, 124.
35 J. Xue, Q. Zheng, Y.Y. Wei, K.J. Yuan, Z. Li, H.H. Wang, *Ind. Eng. Chem. Res.*, 2012, **51**, 4703.
36 Z.G. Wang, H. Liu, X.Y. Tan, Y.G. Jin, S.M. Liu, *J. Membr. Sci.*, 2009, **345**, 65.
37 L. Wang, S. Imashuku, A. Grimaud, D. Lee, K. Mezghani, M.A. Habib, Y. Shao-Horn, *ECS Electrochem. Lett.*, 2013, **2**, F77.
38 S. Imashuku, L. Wang, K. Mezghani, M.A. Habib, Y. Shao-Horn, *J. Electrochem. Soc.*, 2013, **160**, E148.
39 S. Lubke, H.-D. Wiemhofer, *Ber. Bunsenges. Phys. Chem.*, 1998,**102**, 642.
40 B. CH Steele, Curr. Opin. Solid State Mater. Sci., 1996, **1**, 684.
41 R.V. Mangalaraja, S. Ananthakumar, M. Paulraj, K. Uma, M. López, C.P. Camurri, R. E. Avila, *Process. Appl. Ceram.*, 2009, **3**, 137.
42 H. Yahiro, Y. Eguchi, K. Eguchi, H. Arai, *J. Appl. Electrochem.*, 1988, **18**, 527.
43 J. Liu, W. Weppner, *Ionics*, 1999, **5**, 115.
44 M. Arnold, H.H. Wang, J. Martynczuk, A. Feldhoff, *J. Am. Ceram. Soc.*, 2007, **90**, 3651.
45 W. Wang, C. Su, Y.Z. Wu, R. Ran, Z.P. Shao, *Chem. Rev.*, 2013, **113**, 8104.